Computational Materials Science 67 (2013) 151–155

Contents lists available at SciVerse ScienceDirect

Computational Materials Science

journal homepage: www.elsevier.com/locate/commatsci

Comparison of band profiles and magnetic properties of the different phases of $BaTbO_3$

Zahid Ali [a,b], Iftikhar Ahmad [a,*], S. Jalali Asadabadi [c]

[a] Materials Modeling Center, Department of Physics, University of Malakand, Chakdara, Pakistan
[b] Department of Physics, Hazara University, Mansehra, Pakistan
[c] Department of Physics, Faculty of Science, University of Isfahan, Hezar Gerib Avenue, Isfahan 81744, Iran

ARTICLE INFO

Article history:
Received 5 July 2012
Accepted 1 September 2012
Available online 5 October 2012

Keywords:
Perovskites-oxides
Density functional theory
Electronic band structures
Magnetic properties

ABSTRACT

The full potential linearized augmented plane wave (FP-LAPW) method within the frame work of the density functional theory is used to study $BaTbO_3$ in three different phases; cubic (space group *pm-3m*), tetragonal (*I4/mcm*) and orthorhombic (*Ibmm*). The calculated structural parameters and geometries are found in agreement with the experimental results. The spin polarized electronic band structures and densities of states for all the three phases demonstrate that $BaTbO_3$ is insulator. The insulating nature of the material is consistent with the experiments and contradicts with the theoretical results of the metallic behavior and narrow band gap semiconductor. Furthermore, the calculated magnetic moment of Tb^{4+} is in close agreement with the experiments. This comprehensive theoretical study provides a realistic theoretical approach to understand $BaTbO_3$ in its different phases.

1. Introduction

Perovskite oxides have attracted enormous attention in the recent years because of their efficient use in solid fuel cells, gas separation membranes, chemical reactors, high temperature superconductivity, ferroelectricity, piezoelectricity and so forth [1,2]. One of the interesting members of the perovskite oxides family is $BaTbO_3$, which exists in three different phases cubic, tetragonal and orthorhombic phases.

$BaTbO_3$ is an insulating material and due to its compatibility with $YBa_2Cu_3O_{7-x}$ it is an efficient material for high temperature superconductivity [3,4]. Fu et al. [5] used high-resolution neutron powder diffraction technique and reported that $BaTbO_3$ has different phase transitions. Below 260 K $BaTbO_3$ exists in orthorhombic structure possessing space group *Ibmm*, at 373–573 K it occurs in tetragonal symmetry (space group *I4/mcm*), while it adopts cubic phase (*Pm-3m*) at 623 K [5,6]. Jacobson et al. [4] reported the rhombohedral structure of $BaTbO_3$ with space group R-3c. Tezuka et al. [7] observed the rhombohedral (*R-3c*) to orthorhombic (*Pnma*) phase transition in $BaTbO_3$ with the decrease of temperature, from room temperature to 10 K.

The neutron diffraction and magnetic susceptibility measurements show that in $BaTbO_3$ perovskite, Tb^{4+} (f^7) is octahedrally coordinated [8]. $BaTbO_3$ compound shows anti-ferromagnetic transition with valuable magnetic moment 7.99 μ_B of terbium (Tb^{4+}) [9]. $BaTbO_3$ becomes an anti-ferromagnetic material with simple G-type order at 37 K. The Tb^{4+} form factor is also determined by neutron diffraction experiments on a polycrystalline sample at 4.2 K [8].

Several groups have performed experimental and theoretical studies on the electronic structure and magnetic properties of $BaTbO_3$. Hojezyk et al. [3] experimentally studied $BaTbO_3$ and suggest that it is an insulating material with great potentials for high temperature superconductor devices. Poppe et al. [10] studied cubic $BaTbO_3$ and reported that it is an insulating material and could be an efficient dielectric material in field effect devices. Gao et al. [11] used the density functional theory (DFT) with plane wave pseudopotential (PWPP) method and predicted that $BaTbO_3$ is metallic in nature. Chunlan et al. [12] used linear muffin-tin orbitals within atomic-sphere approximation (LMTO-ASA) method and reported that $BaTbO_3$ is a narrow bandgap semiconductor with a band gap of 0.61 eV.

As the reported theoretical studies [11,12] do not agree with the experimental results and therefore the problem needs to be revisited theoretically with a more effective technique which can provide better results, consistent to the experimental ones. In the present DFT studies, the problem is revisited with the full potential linearized augmented plane waves (FP-LAPW) method having exchange correlation of Perdew–Burke–Ernzerhof generalized gradient approximation (PBE-GGA) with the extension of U (GGA + U). The ground state structural parameters, geometries, electronic band structures and total and partial densities of states (DOSs) of $BaTbO_3$ perovskite are investigated in three different phases (cubic, tetragonal and orthorhombic).

* Corresponding author. Address: Department of Physics, University of Malakand, Chakdara, Dir (L), Pakistan. Tel.: +92 332 906 7866.
E-mail address: ahma5532@gmail.com (I. Ahmad).

0927-0256/$ - see front matter © 2012 Elsevier B.V. All rights reserved.
http://dx.doi.org/10.1016/j.commatsci.2012.09.001

2. Computational details

In the present work Kohn–Sham equations [13] are solved to calculate the structural, electronic and magnetic properties of $BaTbO_3$. The details of the spin-polarized FP-LAPW method, formulas and the WIEN2k software used in the present calculations can be found in Ref. [14].

In order to calculate the electronic and magnetic properties of $BaTbO_3$ by GGA + U, it is assumed that the density matrix is diagonal and U is the same for all Coulomb interactions ($U_{ij} \equiv U$) and J is also the same for all exchange interactions ($J_{ij} \equiv J$). There are several methods to incorporate the U-term, [15,16] but here the self-interaction correction (SIC) introduced by Anisimov and coworkers [17] as implemented in the WIEN2k package is used. In the GGA + U^{SIC} methods the total energy is

$$E = E_0 + E_{GGA+U^{SIC}} \tag{1}$$

In Eq. (1), E_0 is defined to be $T_{S,0} + E_{ei} + E_H + E_{ii} + E_{XC}$, where $T_{S,0}$, E_{ei}, E_H, E_{ii} and E_{XC} are the kinetic energy, Coulomb electron–nuclei interaction, Hartree energy, nuclei–nuclei Coulomb interaction, and exchange–correlation energy, respectively.

$$E_{GGA+U^{SIC}} = \frac{U-J}{2}\left(N - \sum_{m,\sigma} n_{m,\sigma}^2\right) \tag{2}$$

In Eq. (2), N is the total number of electrons and $n_{m,\sigma}$ is the occupation number of $|l, m, \sigma\rangle$ state with spin σ. An approximated correction value of U–J for the SIC is probably the best for strongly correlated systems and, as recommended in Ref. [14], for a full potential method we use an "effective" $U_{eff} = U$–J by setting $J = 0$.

After examining and testing several values of Hubbard potential in order to adjust the Tb-4f orbitals level in the density of states, the final Hubbard potential used is $U_{eff} = U$–$J = 4.0$ eV for U.

The core electrons are treated fully relativistically and the valence electrons are treated semi-relativistically. In order to ensure that no electron leakage is taking place semi-core states are included so that accurate results can be achieved; 2300 k-points are used and R_{MT} $K_{max} = 8.00$ determines the plane wave basis functions.

3. Results and discussions

3.1. Structural properties

The unit cells for all the three phases of $BaTbO_3$ i.e. cubic, tetragonal and orthorhombic are presented in Fig. 1. Each unit cell is optimized like in our previous works [1,2,18,19]. The ground state structural parameters are evaluated from the optimum volumes (optimization plots are not given). The calculated lattice constants, bulk moduli, pressure derivative of the bulk moduli and ground state energies from the optimum volume are presented in Table 1. It can be deduced from the table that the calculated lattice constants are underestimated from the experimental results by 0.46%,

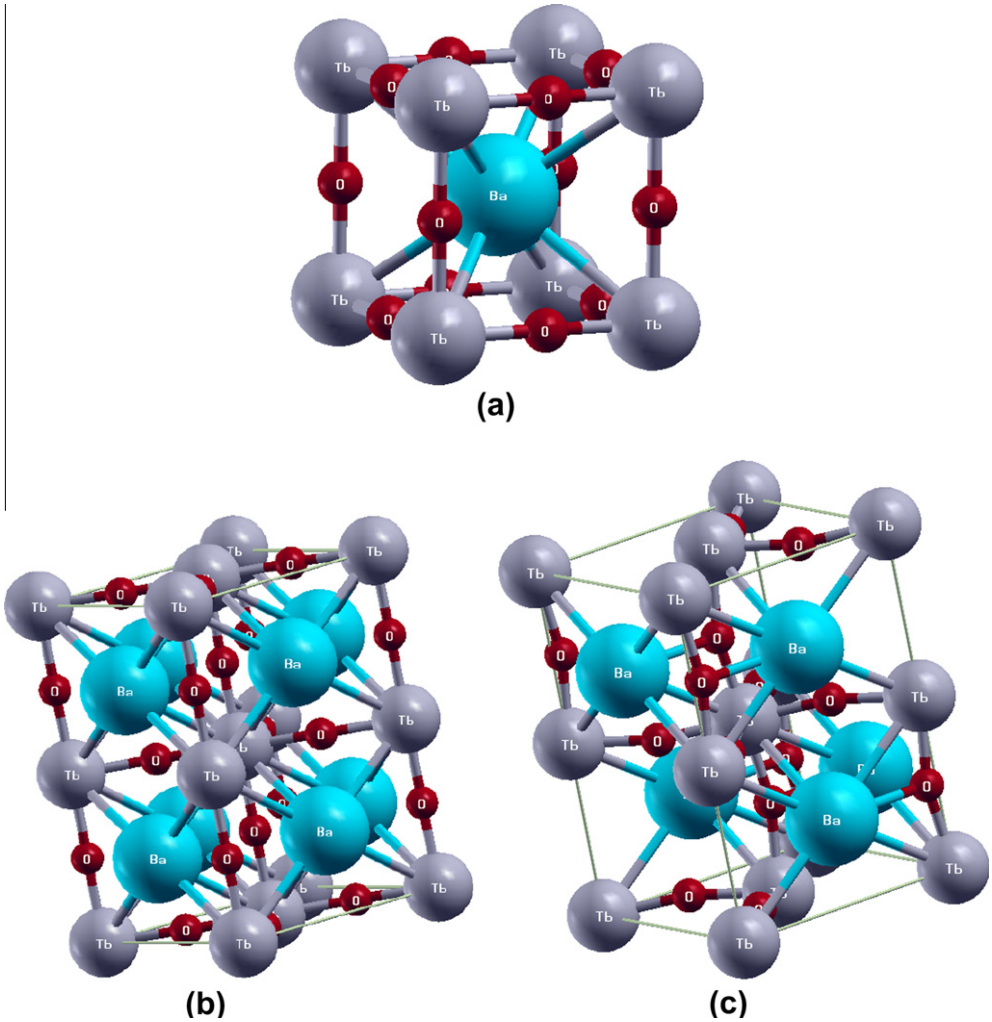

Fig. 1. Crystal structure of $BaTbO_3$ (a) cubic space-group no.221 (*pm-3m*) (b) tetragonal space-group no.140 (*I4/mcm*) (c) orthorhombic, space-group no. 74 (*Ibmm*).

Table 1
Calculated and experimental values of the lattice constants, ground state energies, bulk moduli, derivative of bulk moduli, bonds lengths and bonds angles of the cubic, tetragonal and orthorhombic $BaTbO_3$ in G-type antiferromagnetic, paramagnetic and ferromagnetic magnetic phases.

$BaTbO_3$	Present (DFT)	Experimental	Other
Cubic			
Lattice constant (Å)	4.28	4.30[a,b,c]	4.24[d], 4.27[e]
Ground state energy (Ry)			
$E_{0\ G\text{-}AFM}$	−40164.8041		
$E_{0\ para}$	−40154.6034		
$E_{0\ FM}$	−40160.4265		
Bulk moduli (GPa)	123.5648		
B'	5.000		
Bond length (Å)			
Ba–O	3.026		
Ba–Tb	3.706		
Tb–O	2.14	2.15[f]	
Tetragonal			
$a = b$ (Å)	5.9355	6.061[g]	
c (Å)	8.417	8.595[g]	
Ground state energy (Ry)			
$E_{0\ G\text{-}AFM}$	−80329.7299		
$E_{0\ para}$	−80218.5423		
$E_{0\ FM}$	−80223.9457		
Bulk moduli (GPa)	150.6661		
B'	5.000		
Bond length (Å)			
Ba–O(1)	3.022	3.0241[f]	
Ba–O(2)	3.1767	3.21[f]	
Ba–O(2)	2.8230	2.84[f]	
Ba–Tb	3.7146		
Tb–O(1)	2.1469	2.1464[f]	
Tb–O(2)	2.1515	2.1548[f]	
Bond angle (°)			
Tb–O(1)–Tb	180.000		
Tb–O(2)–Tb	169.4874		
Orthorhombic			
a (Å)	5.9370	6.0714[f]	
b (Å)	5.9103	6.0440[f]	
c (Å)	8.3368	8.5256[f]	
Ground state energy (Ry)			
$E_{0\ G\text{-}AFM}$	−80306.9435		
$E_{0\ para}$	−80297.6034		
$E_{0\ FM}$	−80302.8623		
Bulk moduli (GPa)	207.8058		
B'	5.000		
Bond length (Å)			
Ba–O(1)	3.0390		
Ba–O(2)	3.1689		
Ba–Tb	3.7054		
Tb–O(1) (Å	2.1536		
Tb–O(2)	2.1534		
Bond angle (°)			
Tb–O(1)– Tb	165.4546		
Tb–O(2)–Tb	169.1614		

[a] Ref. [3].
[b] Ref. [10].
[c] Ref. [4].
[d] Ref. [11].
[e] Ref. [12].
[f] Ref. [6].
[g] Ref. [5].

2.07% and 2.21% for the cubic, tetragonal and orthorhombic phases, respectively. The small differences between the experimental and theoretical lattice constants reveal the reliability of our theoretical work.

Bonds length and bonds angle play important role in the symmetry of a crystal. Keeping in view the importance of these parameters, bonds length between different atoms in the cubic, tetragonal and orthorhombic phases are calculated and presented in Table 1. The bond length for Tb–O in the cubic phase is 3.026 Å, for tetragonal Tb–O(1) is 2.1469 Å and Tb–O(2) is 2.1515 Å and for orthorhombic Tb–O(1) is 2.1536 Å and Tb–O(2) is 2.1534 Å. In tetragonal and orthorhombic phases the two different bond lengths between Tb and O is because of the two different positions of O in the crystals. The calculated bonds lengths between other atoms are also presented in the table. It is clear from the table that our calculated bonds lengths are in close agreement with the available experimental results. The calculated bond angle between Tb–O(1)–Tb is 180° and Tb–O(2)-Tb is 169.4878° for tetrahedral structure, while the bond angle between Tb–O(1)-Tb is 165.4546° and Tb–O(2)–Tb is 169.1614° for the orthorhombic structure.

3.2. Electronic properties

The electronic properties of $BaTbO_3$ in the cubic, tetragonal structures are revealed by investigating the calculated spin-polarized electronic band structures, plotted in Fig. 2. The overall band profiles for all the three phases are almost similar to each other. The spin up state for the cubic phase is presented in Fig. 2a. It is clear from the figure that a wide band gap (5.02 eV) exists at Γ symmetry point and hence the material is insulator. While a similar trend is also observed for the spin up state of the tetragonal phase of the compound. A careful analysis of Fig. 2a and c reveals difference in the atomic orbitals and in the energy band gaps. This is due to the difference in the crystal structures and number of atoms per unit cell. The band structure for the spin down states of the cubic phase is shown in Fig. 2b. By comparing Fig. 2a with Fig. 2b, one notices that the band structure for spin down states, as shown in Fig. 2b, can be nearly obtained from the band structure of the spin up states. This can be performed by moving upward the valance bands for spin up electrons, as shown in Fig. 2a, towards higher energies while keeping the conduction bands unchanged. In this way, one can imagine that the Tb f-states are shifted from the topmost valance bands in the vicinity of Fermi level, as shown in Fig. 2a, to the conduction bands which are now far from the Fermi level, as shown in Fig. 2b. Therefore, even then a large band gap, i.e., 4.4 eV, exists in the down band structure at the same symmetry point. Hence, the compound remains insulator for the spin down channel too. A similar trend is observed for the spin down states of the compound for the tetragonal phase shown in Fig. 2d. The band profile and gap of the orthorhombic $BaTbO_3$ are similar to the tetragonal phase and hence are not presented here.

The spin polarized total and partial density of states DOSs for $BaTbO_3$ in the cubic, tetragonal and orthorhombic phases are calculated to explain the origin of the electronic bands and reveal the contribution of different orbitals in the band structures. The calculated DOSs are plotted in Figs. 3 and 4. Fig. 3 displays total and partial DOS for the cubic phase of the compound. In case of spin up state, the bottom of the valance band is occupied by the Tb-5p states in the range −22 to −18.4 eV. At −9 eV the contribution of Ba-5p state takes place. O-2p state occurs in the range −6.3 to −3.6 eV, while Tb-4f state is localized before the Fermi level for all the three phases. In conduction band the main contributions are due to the unoccupied states of Ba-5d and 4f. In conduction band minimum (CBM) peak is due to the unoccupied 4f states of Ba. A wide gap exists between the valance band maximum (VBM) and the CBM which makes the compound wide band gap insulator (5.02 eV). In case of spin down state the Tb-5p state shift forward in the valance band, ranges from −20 to −14 eV, 2p state of O shifts near the Fermi level forming valance band, while the 4f state of Tb jumps in the conduction band and is localized at 4 eV. Again a large gap exists between the valance and conduction band (4.4 eV). Similarly Fig. 4 explains the band structure of the tetragonal phase. Similar results are also observed for orthorhombic phase (figure not given). For all the three phases, spin polarization has been observed but even then wide band gap exists around the Fermi level. Hence our spin polarized theoretical calculations show that

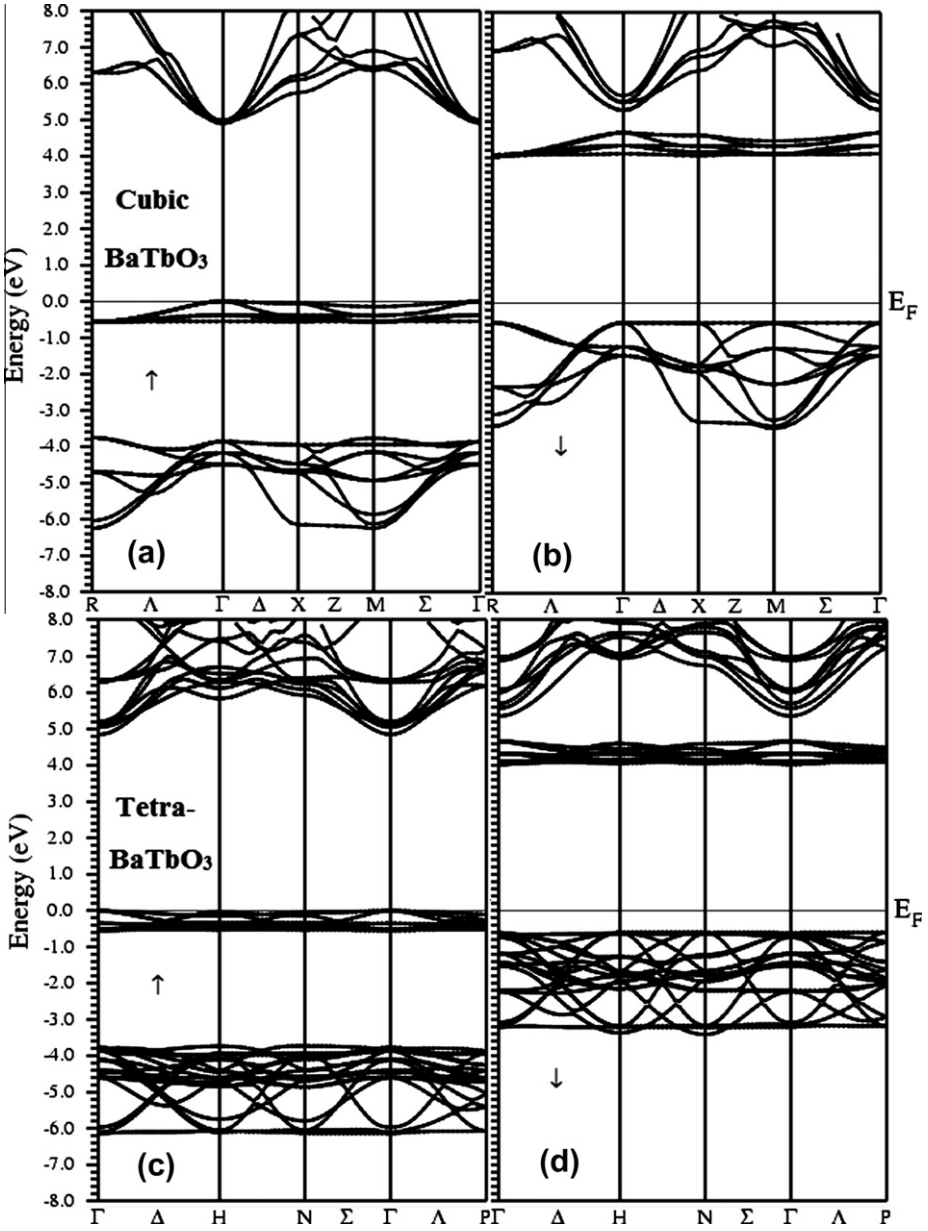

Fig. 2. Electronic band structure for cubic and tetragonal $BaTbO_3$.

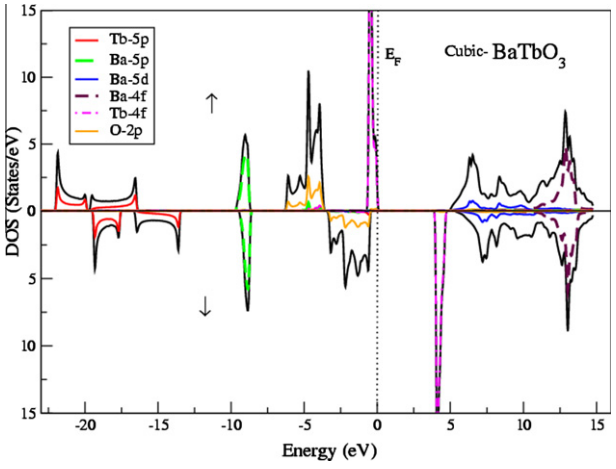

Fig. 3. Total and partial DOSs for cubic $BaTbO_3$.

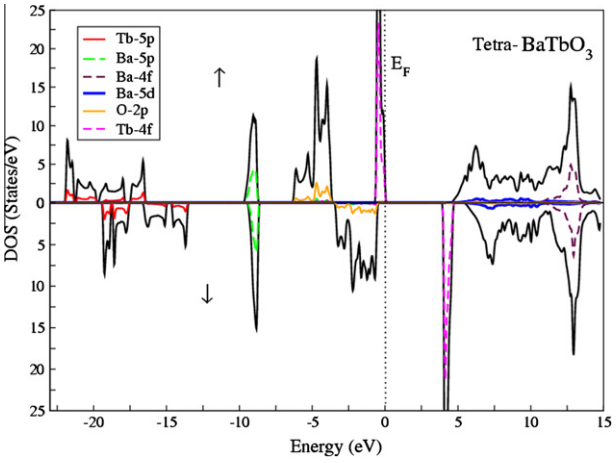

Fig. 4. Total and partial DOSs for orthorhombic $BaTbO_3$.

Table 2
Calculated effective magnetic moment of Tb in unit of (μ_B) per unit cell for the cubic, tetragonal and orthorhombic $BaTbO_3$.

$BaTbO_3$	Present (DFT)	Experimental	Other
Cubic			
M^{Tb}	6.2764	6.50[a]	5.83[b]
Tetragonal			
M^{Tb}	6.4033		
Orthorhombic			
M^{Tb}	6.3972	6.5[c]	

[a] Ref. [7].
[b] Ref. [12].
[c] Ref. [4].

$BaTbO_3$ is insulator which agrees with the reported experimental work [3] and contradicts with the other theoretical studies, narrow band gap semiconductor [12] and metal [11].

3.3. Magnetic properties

The magnetic properties of $BaTbO_3$ are investigated in three different phases, cubic, tetragonal and orthorhombic. The stable magnetic state of each phase is evaluated by calculating the total ground state energy verses volume per unit cell for the paramagnetic, ferromagnetic and G-type anti-ferromagnetic states. The calculated ground state energy per unit cell for all the three phases are presented in Table 1. It is clear from the table that the stable magnetic state of the compound is G-type anti-ferromagnetic for which the ground state energy of $BaTbO_3$ is lower as compared to the paramagnetic and ferromagnetic states. In this regard our theoretical calculations are in agreement with the available experimental and theoretical results [4,7,8,12].

In perovskites, anti-ferromagnetic temperature orders for rare-earth compounds are low as compared to the compounds possessing transition elements [20]. Hutchings et al. [21] studied the exchange coupling for f^7 ions and concluded that the superexchange process is complicated due to the spin polarization of the 5s and 5p orbitals. As a result, a large number of contributions to the exchange energy have to be included, showing covalency terms involving in 5p electrons [22]. In $BaTbO_3$ the 4f orbitals of Tb^{4+} are closer in energy to Tb-5s, Tb-5p and O-2p electrons. The G-type anti-ferromagnetic order in $BaTbO_3$ shows that the approximately linear Tb^{4+}–O^{-2}–Tb^{4+} exchange is dominant as compared to 90° exchange, which is not possible in the perovskite structures [8]. In $BaTbO_3$ and even in TbO_2 the metal–oxygen–metal (Tb^{4+}–O^{-2}–Tb^{4+}) link is tetrahedral magnetic order. The high ordering temperature of $BaTbO_3$ is therefore consistent with both increased covalency, spin polarization and with the favorable 180° superexchange.

The magnetic behavior of $BaTbO_3$ is examined especially the magnetic moment of Tb for all the three different phases. The calculated magnetic moments are presented in Table 2. It is obvious from the table that our calculated magnetic moment of Tb for the cubic phase is 6.27 μ_B, which is 3.3% different from the experimentally measured value (6.50 μ_B) [7]. The comparison with the other theoretical calculated result (5.83 μ_B) reported in Ref. [12] shows that our result is 7.1% closer to the experiments. The calculated magnetic moment of Tb for tetragonal phase is 6.4 μ_B and for orthorhombic phase is 6.39 μ_B. It is also obvious from the table that the effective magnetic moment of Tb for the orthorhombic phase is also consistent with the experimentally reported work [4].

4. Conclusions

In summary, we have theoretically revisited the electronic properties of the $BaTbO_3$ in three different phases using the full potential linearized augmented plane waves (FP-LAPW) method. The calculated spin-polarized electronic band structures of the compound in all the three phases show that the material is insulator. The insulating nature of the material agrees with the experiments while contradicts with the earlier theoretical findings where in one studies it is reported metallic and in another study it is predicted narrow bandgap semiconductor.

The structural parameters and geometries are found consistent with the experimental results. The calculated total and partial densities of states show the contribution of different electronic levels in the band structure. Furthermore, the magnetic nature and properties of the compound are also evaluated and the calculated magnetic moment of Tb^{4+} is found in close agreement with the experimental results.

References

[1] G. Murtaza, I. Ahmad, B. Amin, A. Afaq, M. Maqbool, J. Maqssod, I. Khan, M. Zahid, Opt. Mater. 33 (2011) 553.
[2] Z. Ali, I. Ahmad, B. Amin, M. Maqbool, G. Murtaza, I. Khan, M.J. Akhtar, F. Ghaffor, Physica B 406 (2011) 3800.
[3] R. Hojezyk, C.L. Jia, U. Poppe, K. Urban, Physica C 731 (1997) 282.
[4] A.J. Jacobson, B.C. Tofield, B.E.F. Fender, Acta Crystallogr. B 28 (1972) 956.
[5] W.T. Fu, D. Visser, K.S. Knight, D.J.W. Ijdo, J. Solid State Chem. 177 (2004) 166.
[6] W.T. Fu, D. Visser, D.J.W. Ijdo, J. Solid State Chem. 165 (2002) 393.
[7] K. Tezuka, Y. Hinatsu, Y. Shimojo, Y. Morii, J. Phys.: Condens. Matter 10 (1998) 11703.
[8] B.C. Tofield, A.J. Jacobson, B.E.F. Fender, J. Phys. C: Solid State Phys. 5 (1972) 2887.
[9] Y. Hinatsu, J. Solid State Chem. 100 (1992) 136.
[10] U. Poppe, R. Hojczyk, C.L. Jia, M.I. Faley, W. Evers, F. Bobba, K. Urban, C. Horstmann, R. Dittmann, U. Breuer, H. Holzbrecher, Appl. Supercond. 9 (1999) 3452.
[11] G.Y. Gao, K.L. Yao, Z.L. Liu, Can. J. Phys. 84 (2006) 115.
[12] M. Chunlan, Y. Ling, Y. Zhongqin, J. Phys.: Condens. Matter 17 (2005) 7963.
[13] W. Kohn, L.S. Sham, Phys. Rev. A 140 (1965) 1133.
[14] P. Blaha, K. Schwarz, G.K.H. Madsen, D. Kvasnicka, J. Luitz, WIEN2K: An Augmented Plane Wave + Local Orbital Program for Calculating Crystal Properties, Techn Universitat, Wien, Austria, 2001.
[15] A.G. Petukhov, I.I. Mazin, Phys. Rev. B 67 (2003) 153106.
[16] P. Novak, J. Kunes, L. Chaput, W.E. Pickett, Phys. Status Solidi B 43 (2006) 563.
[17] V.I. Anisimov, I.V. Solovyev, M.A. Korotin, M.T. Czyzyk, G.A. Sawatzky, Phys. Rev. B 48 (1993) 16929.
[18] B. Amin, S. Arif, I. Ahmad, M. Maqbool, R. Ahmad, S. Goumri-Said, K. Prisbrey, J. Elec. Mater. 40 (2011) 1428.
[19] S. Arif, I. Ahmad, B. Amin, Int. J. Quantum Chem. 112 (2012) 882.
[20] P.W. Anderson, Phys. Rev. 86 (1952) 694.
[21] M.J. Hutchings, R.J. Birgenau, W.P. Wolf, Phys. Rev. 168 (1968) 1026.
[22] R.E. Watson, A.J. Freeman, Phys. Rev. 156 (1967) 251.